16th World Conference on Earthquake Engineering, 16WCEE 2017
Santiago Chile, January 9th to 13th 2017
Paper N° XXXX (Abstract ID)
Registration Code: S-XXXXXXXX

Analytical prediction of the seismic behavior of RC columns with a lumped plasticity model including shear forces

E. Osorio[1], J. M. Bairán[2], A.R. Marí[3]

[1] *Assistant Professor, Facultad de Ingeniería Civil, Universidad Antonio Nariño, e.osorio@uan.edu.co / eosoriob@yahoo.com*
[2] *Associate Professor, Department of Civil and Environmental Engineering, Universitat Politècnica de Catalunya (UPC), Jesus.Miguel.Bairan@upc.edu*
[3] *Full Professor, Department of Civil and Environmental Engineering, Universitat Politècnica de Catalunya (UPC), Antonio.Mari@upc.edu*

Abstract

Under the seismic action, columns are subjected to flexo - compression, shear, and sometimes to torsion. The ductility and strength of reinforced concrete columns may be reduced due to such concurrent forces and moments. Therefore, in the last decade, efforts have been made to predict the behavior of the columns through analytical models that consider the interaction of forces and moments. Recently, the authors developed a model that considers the effects of shear at the material, cross-sectional and member levels in order to be used in concentrated plasticity models. Hence, the effects of shear are accounted for in the confining stress, moment-curvature relationship and in the plastic hinge length. In this paper, the validation of the proposed model has been extended by matching the analytical results with experimental data of columns with brittle shear behavior found in scientific literature. The results of the proposed analytical model properly simulate the behavior of columns with shear failure.

Keywords: seismic behavior, capacity curve, nonlinear response, reinforced concrete, plastic hinge length

1. Introduction

Under the seismic action, reinforced concrete columns can be subjected to combined forces and moments. The constituent materials —concrete, longitudinal and transverse reinforcements— provide joint resistance to the flexo-compression, shear and torsion forces produced by the columns. For example, the transverse reinforcement resists the shear force and simultaneously confines the concrete core, thereby increasing its strength and ductility. Similarly, the longitudinal reinforcement and the concrete participate in the flexo-compression and the shear resisting mechanism at the same time. However, although these concurrent mechanisms are known, their analytical prediction is complex. First of all, the sectional analysis was formulated by taking into account only normal strains of the transverse section. Currently, strategies and formulations have been proposed to account for tangential strains [1-14], but in order to be solved, they require refined analysis methods.

Recently, Osorio, et al. [15] developed an analytical model in order to simulate the effects of bidirectional shear forces in columns under seismic loads. The strategy of this model is to analyze the effects of the shear forces at the material, section and member levels. Consequently, analytical expressions were derived to account for these effects in the concrete stress-strain relationship, the moment-curvature relationship and the plastic hinge length. The capacity curve can be obtained by analyzing the shear effects as a whole at each of the three levels. The advantage of this model is that it can be included in the lumped plasticity or spread plasticity models. In this paper, the fundamental hypotheses of the proposed model are provided and validated using experimental results in columns with shear failure under unidirectional lateral loads.

2. Shear - flexure interaction model hypotheses

The hypotheses for the formulation of the interaction model are provided below, and the effects of the shear forces at the material, section and member levels are analyzed.

2.1 Effect of shear forces on strength and ductility of the confined concrete

Confinement increases concrete strength and ductility. The confinement in the reinforced concrete columns is provided by distributing transverse reinforcement in the form of spirals, hoods or strirrups. Currently, the compressive strength of the confined concrete in a column is determined by assuming that the column is subjected only to uniaxial compression forces. Therefore, it is necessary to take into account the full mechanical capacity to measure the confinement stresses.

However, in a state of flexo-compression and shear combined stresses, the transversal reinforcement resists the shear force, thereby reducing the mechanical capacity of the transversal reinforcement to confine the concrete. Fig. 1 shows the static equilibrium diagram from which the effective confinement stresses can be derived. See Eq. (1), where A_{st} is the area of the stirrups or the spiral, f_{ym} is the yielding strength of the stirrups, σ_{su} is the stress on the transverse reinforcement under shear forces, s is the stirrups spacing, D_c is the center-to-center diameter of the stirrups, and α is a factor that represents the confinement efficiency, which depends on the cross section and the stirrups and their spacing regarding the edge.

$$\sigma_e = \alpha \frac{A_{st} \cdot (f_{ym} - \sigma_{su})}{s \cdot D_c} \qquad (1)$$

An asymmetric confinement state provides less strength and ductility capacity than that provided by symmetric confinement stresses. The confined concrete capacity under asymmetric confinement stresses can be assessed with the Mander et al. model [16].

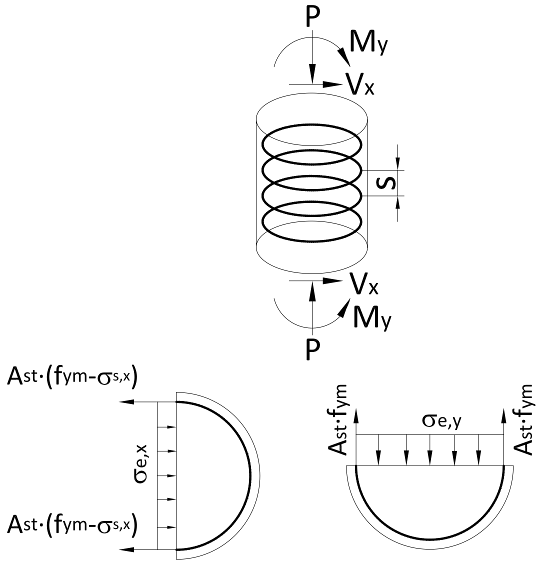

Fig. 1 Effect of shear forces in the confinement stresses [15]

2.2 Effect of shear forces on the longitudinal reinforcement

In a shear strength strut-and-tie model, the shear force is equilibrated with the longitudinal reinforcement, thereby increasing the tensile force on the longitudinal reinforcement. In its ultimate state, this mechanism reduce flexural capacity and increases the plastic hinge length. Based on the equilibrium and disregarding the contribution of the concrete to the shear strength, the decrease in the flexure strength capacity (ΔM_v) can be obtained. See Eq. (2).

$$\Delta M_v = \Delta T \cdot z = \frac{1}{2}\frac{\left(V_d - V_p\right)^2}{\sum \frac{A_s}{s} f_{yt}} \qquad \forall\, V_d \geq V_p \tag{2}$$

Where, ΔT is the increment in the tensile force at the transverse reinforcement, z is the lever arm, V_d is the shear load, V_p is the contribution of the axial load to the shear strength [17], A_s is the area of the transverse reinforcement, f_{yt} is the tensile force of the mean yielding strength of the transverse reinforcement, and s is the transverse reinforcement spacing.

2.3 Effect of shear forces on the moment-curvature relationship

The effective flexural strength can be obtained as the ultimate bending moment capacity minus the increment in the bending moment from the shear force, as given in Eq. (3).

$$M_{fv} = M_f - \Delta M_v \tag{3}$$

The moment-curvature relationship can be modified to calculate the reduction in each of the load steps. However, for practical purposes, the modified moment-curvature relationship can be approximated by rotating the entire diagram using Eq. (4), as shown in Fig. 2. This way, the shear effects are taken into account in the moment-curvature relationship.

$$M_{fv} = M_f - \Delta M_{v,máx} \frac{M_f}{M_{f,máx}} \quad (4)$$

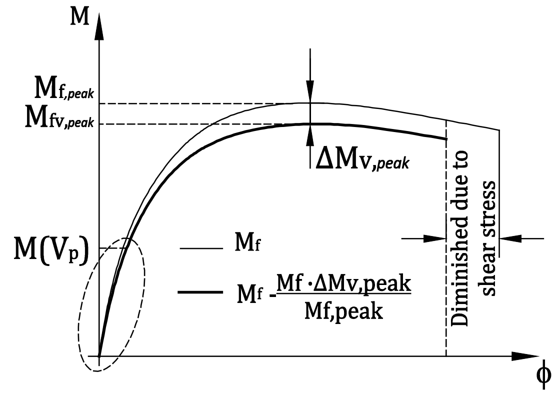

Fig. 2 Moment-curvature relationship rotation to account for the shear effects [15]

2.4 Effect of shear forces on the longitudinal reinforcement

The plastic hinge length is a parameter still under discussion by the scientific community, hence, there is a wide variety of expressions in literature proposed for its quantification. Reference [18; 19] provides a summary of these. However, design recommendations and rules, such as references [20-22], recommend the proposal of Paulay, et al. [23], Eq. (5).

$$L_p = \left(1 - \frac{M_y}{M_{máx}}\right) L + \alpha_b f_y d_b \quad (5)$$

Where, L is the lever arm calculated as L=M/V, d_b is the longitudinal bar diameter, f_y is the yielding strength of the longitudinal reinforcement and, α_b is a coefficient experimentally measured. Paulay and Priestley [23] proposed the values $\left(1 - \frac{M_y}{M_{máx}}\right) = 0.08$ and $\alpha_b = 0.022$, respectively.

Park and Pauly [24] demonstrated that the tensile strength of the longitudinal reinforcement increases when the concrete shear cracks propagated in a diagonal direction. Consequently, the plastic hinge length is also increased. However, the shear force effect in the plastic hinge length proposed in equation Eq. (5) was not included explicitly. The shear force effect can be included in Eq. (5) accounting for the reduction of flexural strength capacity (ΔM_v) previously explained in Eq. (2), and Eq. (6) is obtained. Details of the numerical implementation and formulation of the model are provided in reference [15].

$$L_p = \left(1 - \frac{M_y}{M_{máx}}\right) L + \alpha_b f_y d_b + \frac{1}{2} \frac{\left(V_d - V_p\right)^2}{V_d \sum \frac{A_s}{s} f_{yt}} \quad \forall\, V_d \geq V_p \quad (6)$$

3. Validation examples of the shear-flexure interaction model

In this section, we present the results of the proposed analytical model compared to the experimental measurements of column tests conducted by Arakawa, et al, [25] and Yoshimura, et al. [26]. Arakawa, et al. conducted an experimental campaign of reinforced concrete columns with octagonal cross sections inscribed in a 275-mm-diameter circumference. In the columns under study, the longitudinal reinforcement consisted of 12 bars, each of which had a 16 mm diameter and the transverse reinforcement consisted of 6-mm diameter spirals.

The test configuration corresponds to a double curvature scheme. Other parameters of interest in the modeling are presented in Table 1. The experimental measurement data was consulted in the compilations published in references [27, 28].

Table 1 – Characteristic properties of the columns of Arakawa, et al. [25]

#	Axial load	f'c	fy	fyt	L - Inflection	s	Failure type
	kN	MPa	MPa	MPa	mm	mm	
2	0	29.3	366	368	300	50	Shear
19	215	31.2	363	381	450	75	Shear
28	430	41.3	363	381	450	75	Shear

In Fig. 3, the analytical results of the shear-flexure interaction and flexure-only models are presented, compared to the experimental measurements, Arakawa, et al. [25]. Fig. 3a presents the results for column #2, whose axial load is 0.0 kN. This figure shows that the proposed interaction model replicates the behavior observed experimentally, both in load capacity values and in ductility. There is also a significant reduction in terms of lateral load capacity (approx. 30%) compared to the response when considering a flexure-only model. Fig. 3a presents the results for column #19 and it can be observed how the F-V interaction model properly reflects the measurements taken during the experiments. Fig. 3c presents the results for column #28. It can also be observed that the interaction model approximates the experimental behavior better than the flexure-only model in this column.

Yoshimura, et al. conducted an experimental campaign with rectangular cross sections of 300 x 300 mm^2. Reinforcement consisted of 12 bars, each of which had a 16 mm diameter, and the transverse reinforcement consisted of 6-mm diameter stirrups with no additional cross-ties. The test configuration corresponds to a double curvature scheme. Table 2 presents the specific parameters of each specimen. The experimental measurement data was consulted in the compilations published in references [27, 28].

Table 2 – Characteristic properties of the columns of Yoshimura, et al. [26].

#	Axial load	f'c	fy	fyt	L - Inflection	s	Failure type
	kN	MPa	MPa	MPa	mm	mm	
1	552.6	30.7	402	392	600	100	Shear
3	552.6	30.7	402	392	600	200	Shear
4	828.9	41.3	402	392	600	100	Shear

Fig. 4 shows the analytical results of the shear-flexure interaction models and flexure-only models compared to the experimental measurements obtained by Yoshimura, et al. [26]. In all three analyses, the analytical model represents the reduction of the flexure strength capacity and the predominance of shear failure. However, the displacement capacity of the analytical model is lower compared to the one experimentally measured. This can be the result of a combination of various phenomena presented in the reinforced concrete under seismic loads. In this case, it could be due to the rapid decrease of the bond splitting failure due to the poor confinement magnified by the stirrup shape and the lack of ties. In the analytical model, this phenomenon could be included as an increase of the plastic hinge length as a function of the effective confinement stresses and the shear [15], which we intend to study in the future.

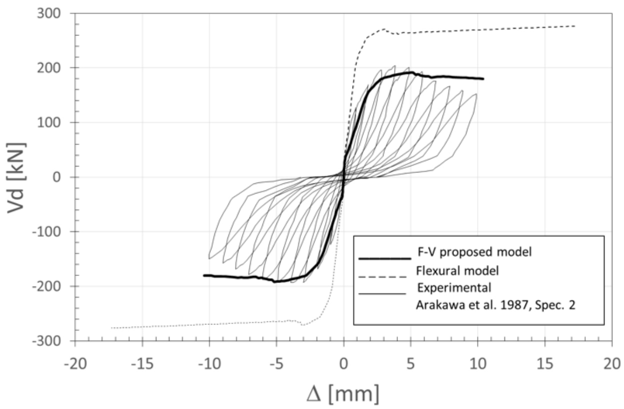

a) Analytical results for column 2

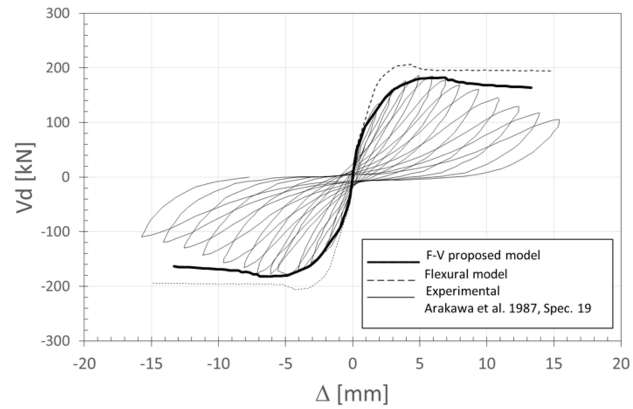

b) Analytical results for column 19

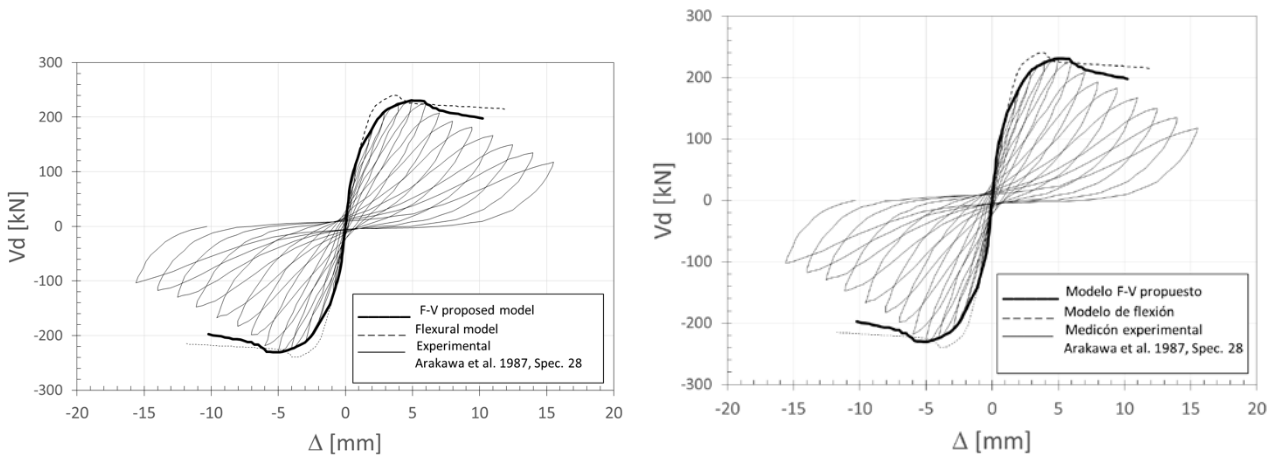

c) Analytical results for column 28

Fig. 3 Comparison between the analytical capacity curves against the experimental data of circular columns

4. Conclusions

In this paper, a Flexure-Shear (F-V) interaction model to simulate the behavior of columns with shear failure is presented. The strategy of this model is to analyze the effects of shear forces at the material, cross-sectional and member levels. The main advantage of the model is that it can be implemented in lumped plasticity models. However, in this F-V interaction model, the cyclic load, laps, the longitudinal bar bending effects, the form and scale effects, among others, have not been included.

The proposed analytical model results were compared to experimental measurements of tests on columns with shear failure. The F-V analytical interaction model replicates the decrease in flexural strength as a consequence of shear effects. The results of the analytical model provide information about the decrease in ductility. In the rectangular columns, it was observed that the displacements of the analytical model are conservative compared to the experimental values, which can be due, among other factors, to a bond mechanism, which we intend to study in the future.

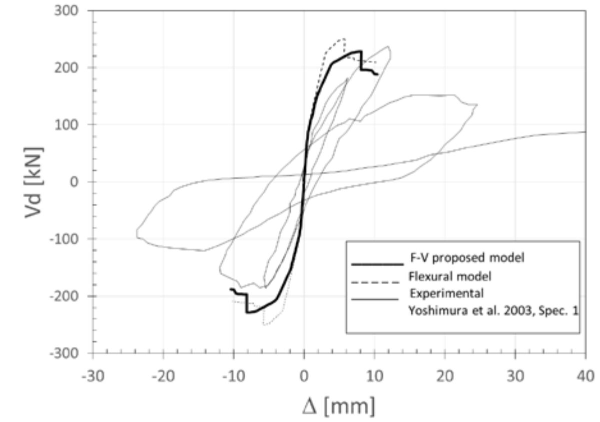

a) Analytical results for column 1

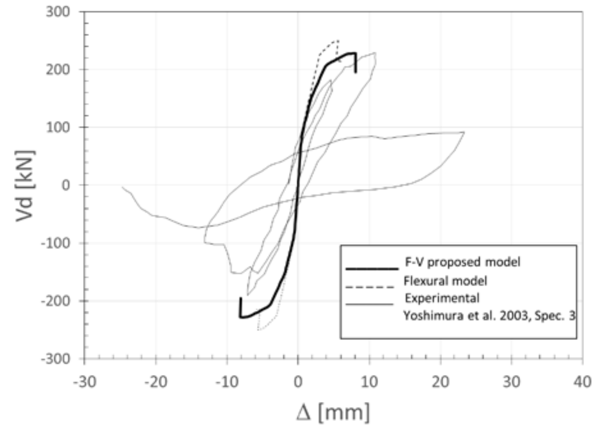

b) Analytical results for column 3

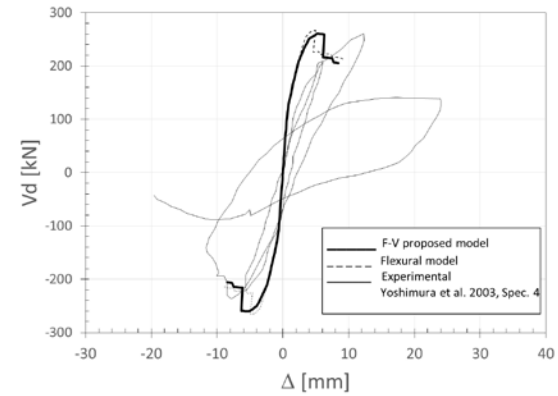

c) Analytical results for column 4

Fig. 4 Comparison between the analytical capacity curves against the experimental data of rectangular columns

5. Acknowledgements

The authors acknowledge the partial financing of projects HORVITAL (BIA2015-64672-C4-1-R) from the Ministry of Economy and Competitiveness Ministry of Spain and project EHMPE (UAN-20141068) from Antonio Nariño University of Colombia.

6. References

[1] P. Ceresa, L. Petrini, R. Pinho (2007): Flexure-Shear Fiber Beam-Column Elements for Modeling Frame Structures Under Seismic Loading — State of the Art, Journal of Earthquake Engineering 11 (2007) 46-88.

[2] J. Navarro, P. Miguel, M.A. Fernández, F.C. Filippou (2007): A 3D numerical model for reinforced and prestressed concrete elements subjected to combined axial, bending, shear and torsion loading, Eng. Structures 29 (2007) 3404-3419.

[3] P. Ceresa, L. Petrini, R. Pinho, R. Sousa (2009): A fibre flexure–shear model for seismic analysis of RC-framed structures, Earthquake Engineering & Structural Dynamics 38 (2009) 565-586.

[4] S. Guner, F. Vecchio (2011): Analysis of Shear-Critical Reinforced Concrete Plane Frame Elements under Cyclic Loading, Journal of Structural Engineering 137 (2011) 834-843.

[5] S.-Y. Xu, J. Zhang (2012): Axial–shear–flexure interaction hysteretic model for RC columns under combined actions, Engineering Structures 34 (2012) 548-563.

[6] L. Martinelli (2008): Modeling Shear-Flexure Interaction in Reinforced Concrete Elements Subjected to Cyclic Lateral Loading, ACI Structural Journal 105 (2008) 675-684.

[7] T.R. Mullapudi, A. Ayoub (2010): Modeling of the seismic behavior of shear-critical reinforced concrete columns, Engineering Structures 32 (2010) 3601-3615.

[8] H. Mostafaei, F. Vecchio (2008): Uniaxial Shear-Flexure Model for Reinforced Concrete Elements, Journal of Structural Engineering 134 (2008) 1538-1547.

[9] D. Ferreira, J. Bairán, A. Marí (2013): Numerical simulation of shear-strengthened RC beams, Engineering Structures 46 (2013) 359-374.

[10] S. Mohr, J.M. Bairán, A.R. Marí (2010): A frame element model for the analysis of reinforced concrete structures under shear and bending, Engineering Structures 32 (2010) 3936-3954.

[11] J.M. Bairan (2005): A non-linear coupled model for the analysis of reinforced concrete sections under bending, shear, torsion and axial forces, Barcelona, Universitat Politècnica de Catalunya, 229.

[12] F.J. Vecchio, M.P. Collins (1988): Predicting the Response of Reinforced Concrete Beams Subjected to Shear using the Modified Compression Field Theory, ACI Structural Journal 85 (1988) 258-268.

[13] E.C. Bentz (2000): Sectional analysis of reinforced concrete members, Toronto, University of Toronto.

[14] J.M. Bairan, A. Mari (2007): Multiaxial-coupled analysis of RC cross-sections subjected to combined forces, Engineering Structures 29 (2007) 1722-1738.

[15] E. Osorio (2012): Effects of cyclic biaxial shear loading on the seismic response of reinforced concrete columns (In spanish), Barcelona, Universitat Politècnica de Catalunya. http://hdl.handle.net/10803/123714

[16] J.B. Mander, M.J.N. Priestley, R. Park (1988): Theoretical Stress-Strain Model for Confined Concrete, Journal of Structural Engineering 114 (1988) 1804-1826.

[17] M.J.N. Priestley, R. Verma, Y. Xiao (1994): Seismic Shear Strength of Reinforced Concrete Columns, Journal of Structural Engineering 120 (1994) 2310-2329.

[18] S. Bae, O. Bayrak (2008): Plastic Hinge Length of Reinforced Concrete Columns, ACI Structural Journal 105 (2008) 290-300.

[19] A. Mortezaei, H.R. Ronagh (2011): Plastic hinge length of reinforced concrete columns subjected to both far-fault and near-fault ground motions having forward directivity, The Structural Design of Tall and Special Buildings (2011) n/a-n/a.

[20] CALTRANS (2013): Caltrans seismic design criteria, version 1.7, Sacramento, CA, California Dept. of Transportation.

[21] AASHTO (2009): Guide specifications for LRFD seismic bridge design, Washington, DC, American Association of State Highway and Transportation Officials.

[22] Eurocode 8 (2012): Design provisions for earthquake resistance of structures : Part 2 Bridges, Madrid, AENOR.

[23] T. Paulay, J.N. Priestley (1992), Seismic Design of Reinforced Concrete and Masonry Buildings, Wiley, 1992.

[24] R. Park, T. Paulay (1975), Reinforced concrete structures, New York, Wiley, 1975.

[25] Arakawa, Takashi; He, Ming-Xuan; Arai, Yasuyuki; and Mizoguchi, Mitsuo (1987): Ultimate Shear Strength of Spirally-Confined Concrete Columns, Transactions of the Japan Concrete Institute, Vol.9, pp. 305-312. Engineering Simulation (database), Dataset, DOI:10.4231/D39Z90B9T.

[26] Yoshimura;M. T.;Y. and Nakamura;T. (2003). Collapse Drift of Reinforced Concrete Columns. The Fifth U.S. - Japan Workshop on Performance-Based Earthquake Engineering Methodology for Reinforced Concrete Structures. Hakone;Japan;Pacific Earthquake Engineering Research Center (UC Berkeley): 239-253.

[27] M.Berry, M. Parrish, M. Eberhard (2004). PEER Structural Performance Database, Pacific Earthquake Engineering Research Center, University of California, Berkeley

[28] W. Ghannoum, B.Sivaramakrishnan (2012). ACI 369 Circular Column Database. Network for Earthquake. Network for Earthquake Engineering Simulation (database), Dataset, DOI:10.4231/D39Z90B9T

[29] W. Ghannoum, B.Sivaramakrishnan (2012). ACI 369 Circular Column Database. Network for Earthquake. Network for Earthquake Engineering Simulation (database), Dataset, DOI:10.4231/D36688J50